Synergistic Cytotoxicity and Pharmacogenetics of Gemcitabine and Pemetrexed Combination in Pancreatic Cancer Cell Lines

Elisa Giovannetti, Valentina Mey, Romano Danesi, et al.

Clin Cancer Res 2004;10:2936-2943.

Featured Article

Synergistic Cytotoxicity and Pharmacogenetics of Gemcitabine and Pemetrexed Combination in Pancreatic Cancer Cell Lines

Elisa Giovannetti, Valentina Mey, Romano Danesi, Irene Mosca, and Mario Del Tacca

Division of Pharmacology and Chemotherapy, Department of Oncology, Transplants and Advanced Technologies in Medicine, Pisa, Italy

Abstract

Purpose: **Gemcitabine is an inhibitor of ribonucleotide reductase (RR) and DNA synthesis and is an effective agent in the treatment of pancreas cancer. The present study investigates whether the multitargeted antifolate pemetrexed would be synergistic with gemcitabine against MIA PaCa-2, PANC-1, and Capan-1 pancreatic cancer cell lines.**

Experimental Design: **Cells were treated with gemcitabine and pemetrexed, and the type of drug interaction was assessed using the combination index. Cytotoxicity of gemcitabine was examined with inhibitors of (*a*) deoxycytidine kinase (dCK), which activates gemcitabine by phosphorylation, and (*b*) 5′-nucleotidase (drug dephosphorylation) and cytidine deaminase (drug deamination), the main inactivating enzymes. The effects of gemcitabine and pemetrexed on cell cycle were analyzed by flow cytometry, and apoptosis was examined by fluorescence microscopy. Finally, quantitative, real-time PCR was used to study the pharmacogenetics of the drug combination.**

Results: **Synergistic cytotoxicity and enhancement of apoptosis was demonstrated, mostly with the sequence pemetrexed→gemcitabine. Pemetrexed increased cells in S phase, the most sensitive to gemcitabine, and a positive correlation was found between the expression ratio of *dCK:RR* and gemcitabine sensitivity. Indeed, pemetrexed significantly enhanced *dCK* gene expression (+227.9, +86.0, and +135.5% in MIA PaCa-2, PANC-1, and Capan-1 cells, respectively), and the crucial role of this enzyme was confirmed by impairment of gemcitabine cytotoxicity after dCK saturation with 2′-deoxycytidine.**

Conclusions: **These data demonstrate that the gemcitabine and pemetrexed combination displays schedule-dependent synergistic cytotoxic activity, favorably modulates cell cycle, induces apoptosis, and enhances dCK expression in pancreatic cancer cells.**

Introduction

In the last decade, the availability of several new active drugs has improved the efficacy of combination regimens and substantially increased the response rate of refractory tumors, including pancreatic cancer (1, 2). Antimetabolites are widely used in combination regimens because of their activity and generally manageable toxicities; however, several preclinical studies have shown schedule-dependent drug interaction (3). For example, gemcitabine (2′,2′-difluoro-2′-deoxycytidine) is synergistic *in vitro* with cisplatin in non-small cell lung cancer cell lines and this interaction is most pronounced when gemcitabine precedes this drug (4, 5). Similar results were obtained using PANC-1 and BxPc3 pancreatic cancer cells for which the most synergistic schedule is gemcitabine followed by cisplatin (6), whereas additive to slightly synergistic or antagonistic effects are observed with gemcitabine followed by topotecan, paclitaxel, and docetaxel in various non-small cell lung cancer cell lines (7–9).

Gemcitabine has a broad spectrum of anticancer activity against solid tumors, and it is an effective agent in the treatment of pancreatic cancer (10). Gemcitabine requires intracellular phosphorylation to its active metabolites, 2′,2′-difluoro-dCDP and 2′,2′-difluoro-dCTP, which, respectively, inhibits ribonucleotide reductase (RR) and is incorporated into the DNA, leading to chain termination (11). The rate-limiting step of drug activation is catalyzed by deoxycytidine kinase (dCK), which phosphorylates gemcitabine, whereas 5′-nucleotidase and cytidine deaminase inactivate gemcitabine by dephosphorylation and deamination, respectively (12). Pemetrexed is a new antimetabolite that inhibits thymidylate synthase, dihydrofolate reductase, and glycinamide ribonucleotide formyltransferase (13), thereby depleting nucleotide pools and blocking DNA synthesis (14, 15). Because of these effects on nucleotide biosynthesis, pemetrexed has the potential to sensitize cells to the cytotoxic activity of gemcitabine. Indeed, the accumulation of cells in the S phase caused by pemetrexed may enhance both gemcitabine incorporation into the DNA and apoptosis (15, 16). Moreover, dCTP depletion and glycinamide ribonucleotide formyltransferase inhibition by pemetrexed may up-regulate dCK, a key enzyme of the nucleotide salvage pathway (14).

For these reasons, the present study was performed in pancreatic cancer cell lines to characterize, from a pharmacological and pharmacogenetic point of view, the combination of pemetrexed and gemcitabine and to provide the experimental basis for potential clinical application of this combination.

Received 11/3/04; revised 12/31/03; accepted 1/16/04.

Grant support: R. Danesi was supported by unrestricted research grants from the Ministero dell'Istruzione, Università e Ricerca (MIUR, Rome, Italy). M. Del Tacca was supported by unrestricted research grants from Eli-Lilly (Florence, Italy).

The costs of publication of this article were defrayed in part by the payment of page charges. This article must therefore be hereby marked *advertisement* in accordance with 18 U.S.C. Section 1734 solely to indicate this fact.

Requests for reprints: Mario Del Tacca, Division of Pharmacology and Chemotherapy, Department of Oncology, Transplants and Advanced Technologies in Medicine, 55, Via Roma, 56126 Pisa, Italy. Phone: 39-050-830148; Fax: 39-050-562020; E-mail: m.deltacca@med.unipi.it.

Materials and Methods

Drugs and Chemicals. Gemcitabine and pemetrexed were generous gifts from Eli Lilly (Indianapolis, IN). Drugs were dissolved in sterile distilled water and diluted in culture medium immediately before use. RPMI and DMEM media, fetal bovine serum, horse serum, L-glutamine (2 mM), penicillin (50 IU/ml), and streptomycin (50 μg/ml) were from Life Technologies, Inc. (Gaithersburg, MD). All other chemicals were from Sigma (St. Louis, MO).

Cell Cultures. MIA PaCa-2 (American Type Culture Collection, Manassas, VA), PANC-1 and Capan-1 cell lines (generous gift of Prof. S. Pedrazzoli and Dr. P. Fogar, University of Padova, Padua, Italy), were grown in DMEM with 10% fetal bovine serum and 2.5% horse serum (MIA PaCa-2), DMEM with 10% fetal bovine serum (PANC-1), and RPMI with 20% fetal bovine serum (Capan-1), glutamine, and penicillin-streptomycin. Cells were cultivated in 75-cm^2 flasks (Costar, Cambridge, MA), at 37°C in 5% CO_2 and 95% air, and were harvested with EDTA when they were in logarithmic growth.

Assay of Cytotoxicity. Cells were plated in 6-well sterile plastic plates (Costar) at 10^5 cells/well and were allowed to attach for 24 h. Cells were treated with (*a*) gemcitabine (0.001–100 μg/ml) for 1 h; (*b*) pemetrexed (0.001–100 μg/ml) for 24 h; (*c*) gemcitabine for 1 h followed by a 24-h washout in drug-free medium and then pemetrexed for 24 h; (*d*) the reverse sequence of point (*c*) above, i.e., cells were treated with a 24-h washout in drug-free medium followed by treatment with gemcitabine for 1 h. After drug treatments were completed, cells were grown for an additional 24 h in drug-free medium, and cytotoxicity was expressed as the percentage of cells surviving relative to untreated cultures; the 50% inhibitory concentration of cell growth (IC_{50}) was calculated by non-linear least squares curve fitting.

Drug interaction between gemcitabine and pemetrexed was assessed, at a concentration ratio of 1:1, using the combination index (CI; Ref. 17), where CI <1, CI = 1, and CI >1 indicate synergistic, additive, and antagonistic effects, respectively. On the basis of the isobologram analysis for mutually exclusive effects, the CI value was calculated as follows:

$$CI = \frac{(D)_1}{(D_x)_1} + \frac{(D)_2}{(D_x)_2}$$

where $(D_x)_1$ and $(D_x)_2$ are the concentrations of pemetrexed and gemcitabine, respectively, required to inhibit cell growth by 50%, and $(D)_1$ and $(D)_2$ are the drug concentrations in combination treatments that also inhibit cell growth by 50% (isoeffective as compared with the single drugs). Data analysis was performed by the Calcusyn software (Biosoft, Oxford, United Kingdom).

Effect of Inhibition of Gemcitabine Metabolism on Cytotoxicity. Cells were plated in 6-well plates as described above and were treated with gemcitabine (0.1 ng/ml to 10 μg/ml) for 24 h, alone or in combination with 2′-deoxycytidine (natural substrate of dCK), tetrahydrouridine (cytidine deaminase competitive inhibitor), and diethylpyrocarbonate (5′-nucleotidase noncompetitive inhibitor), at 10 μM to inhibit drug activation by phosphorylation (dCK), as well as drug inactivation by dephosphorylation (5′-nucleotidase) or deamination (cytidine deaminase), respectively. IC_{50} was calculated as described above.

Cell Cycle Analysis. Cells were plated at 1×10^6 in 100-mm plastic dishes (Costar) and were allowed to attach for 24 h. After treatments with gemcitabine (1 h) and pemetrexed (24 h) alone at their IC_{50} levels, followed by a 24-h washout, cells were harvested with trypsin-EDTA and were washed twice with PBS. DNA was stained with a solution containing propidium iodide (25 μg/ml), RNase (1 mg/ml), and NP40 (0.1%); and samples were kept on ice for 30 min. Cytofluorimetry was performed using a FACScan (Becton Dickinson, San Jose, CA), and data analysis was carried out with CELLQuest software, and cell cycle distribution was determined using Modfit software (Verity Software, Topsham, ME).

Analysis of Apoptosis. Cells were treated with gemcitabine and pemetrexed and their combinations at their IC_{50} levels, as described in "Assay of Cytotoxicity," and, at the end of the incubation, were washed twice with PBS and fixed in 4% buffered paraformaldehyde for 15 min. Cells were resuspended and incubated for an additional 15 min in a solution containing 8 μg/ml bisbenzimide HCl (18). Cells were spotted on glass slides and were examined by fluorescence microscopy (Leica, Wetzlar, Germany). A total of 200 cells from randomly chosen microscopic fields were counted, and the percentage of cells displaying chromatin condensation and nuclear fragmentation relative to the total number of counted cells (apoptotic index) was calculated.

PCR Analysis of *dCK* and *RR*. Total RNA was extracted from cells treated as described above in "Cell Cycle Analysis," using the TRI REAGENT LS. RNA was dissolved in RNase-free water containing 10 mmol/liter DTT and 200 units/ml RNase inhibitor, and measured at $\lambda_{260\ nm}$. One μg of RNA was reverse transcribed at 37°C for 1 h in a 100-μl reaction volume containing 0.8 mM dNTPs, 200 units of moloney murine leukemia virus reverse transcriptase, 40 units of RNase inhibitor, and 0.05 μg/ml random primers. The cDNA was amplified by quantitative real-time PCR with the Applied Biosystems 7900HT sequence detection system (Applied Biosystems, Foster City, CA). quantitative real-time PCR reactions were performed in triplicate using 5 μl of cDNA, 12.5 μl of TaqMan Universal PCR Master Mix, 2.5 μl of probe, and 2.5 μl of forward and reverse primers in a final volume of 25 μl. Samples were amplified using the following thermal profile: an initial incubation at 50°C for 5 min, to prevent the reamplification of carryover-PCR products by AmpErase uracil-*N*-glycosylase, followed by incubation at 95°C for 10 min, to suppress AmpErase uracil-*N*-glycosylase activity and to denature the DNA, 40 cycles of denaturation at 95°C for 15 s followed by annealing and extension at 60° for 1 min.

Forward (F) and reverse (R) primers and probe (P) were designed with Primer Express 2.0 (Applied Biosystems) on the basis of *dCK* gene sequence obtained from the GenBank: 5′-TTC CTG AAC CTG TTG CCA GAT-3′(F); 5′-GAG ACA TTG TAA GTT CCT CAA ATT CAT C-3′(R), and 5′-TGC AAT GTT CAA AGT ACT CA-3′ (P). Primers and probes for the regulatory (*RRM1*) and catalytic (*RRM2*) subunits of *RR* were from Applied Biosystems Assay on-Demand Gene expression products Hs00168784 and Hs0035724. Amplifications were normalized to glyceraldehyde 3-phosphate dehydrogenase (*GAPDH*), and quantitation of gene expression was performed

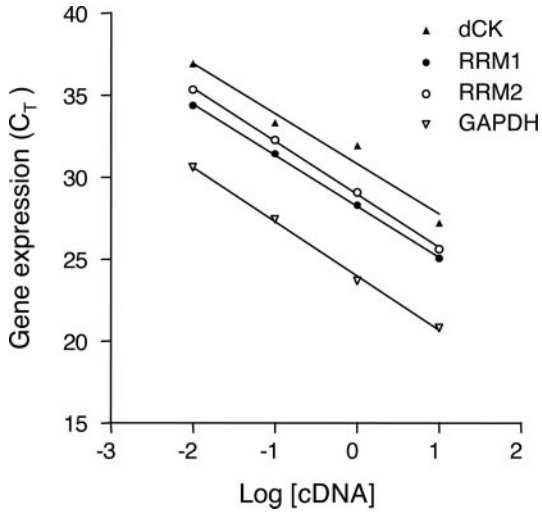

Fig. 1 Deoxycytidine kinase (*dCK*), *RRM1* (regulatory subunit of ribonucleotide reductase), *RRM2* (catalytic subunit of ribonucleotide reductase), and glyceraldehyde 3-phosphate dehydrogenase (*GAPDH*) standard curves for validation of quantitative real-time PCR (QRT-PCR) method. The following equations apply to the target gene amplification: $y = -3.06x + 30.82$, $R^2 = 0.96$ (*dCK*); $y = -3.12x + 28.32$, $R^2 = 0.99$ (*RRM1*); $y = -3.24x + 28.96$, $R^2 = 0.99$ (*RRM2*); $y = -3.32x + 23.96$, $R^2 = 0.99$ (*GAPDH*). y, C_T; x, logarithm of cDNA (mg).

using the $\Delta\Delta C_T$ calculation, where C_T is the threshold cycle; the amount of target gene, normalized to *GAPDH* and relative to the calibrator (untreated control cells), is given as $2^{-\Delta\Delta C_T}$ (19). Optimal primer concentration, *i.e.*, associated with minimum SDs between C_T values, was 300 nM, as preliminarily assessed in PCR reactions with all of the combinations of forward and reverse primers. A validation experiment was performed to demonstrate that the efficiencies of the target (*dCK*, *RRM1*, and *RRM2*) and reference (*GAPDH*) gene amplifications were approximately equal, using a standard curve method with several dilutions of the cDNA sample from untreated control cells. An ideal slope should be −3.32; the values of the slopes of cDNA calibrator relative to C_T were −3.06 for *dCK*, −3.12 for *RRM1*, −3.24 for *RRM2*, and −3.32 for *GAPDH* (Fig. 1). Therefore, PCR efficiencies were 92.2, 94.0, 97.6, and 100%, respectively, for *dCK*, *RRM1*, *RRM2*, and *GAPDH*.

Statistical Analysis. All of the experiments were performed in triplicate and were repeated at least three times. Data were expressed as mean values ± SE and were analyzed by Student's *t* test or ANOVA followed by the Tukey's multiple comparison; the level of significance was $P < 0.05$.

Results

Cytotoxicity of Gemcitabine and Pemetrexed. A dose-dependent inhibition of cell growth was observed with gemcitabine and pemetrexed (Fig. 2), with IC_{50}s of 2.90 ± 0.34 and 1.58 ± 0.40 μg/ml (MIA PaCa-2), 42.21 ± 5.74 and 2.49 ± 0.29 μg/ml (PANC-1), and 4.75 ± 1.07 and 7.33 ± 1.93 μg/ml (Capan-1), respectively. The sequential exposure of cell lines to pemetrexed followed by gemcitabine reduced the IC_{50}s of gemcitabine to 36.10 ± 1.31, 21.50 ± 2.50, and 94.0 ± 5.62 ng/ml in MIA PaCa-2, Capan-1, and PANC-1, respectively, whereas the IC_{50}s of gemcitabine resulting from the reverse sequence were 123.70 ± 1.45, 352.28 ± 43.87, and 748.00 ± 64.32 ng/ml in MIA PaCa-2, Capan-1, and PANC-1 cells, respectively. The calculation of the CI showed synergism at effect levels >30% (fraction of cells affected by the treatments) for both schedules in the three cell lines (Fig. 3), but the degree of synergism obtained with the pemetrexed→gemcitabine sequence was considerably greater than that observed with the reverse schedule (Fig. 3).

Modulation of Drug Metabolism and Gemcitabine Cytotoxicity. A key role for dCK activity on sensitivity to gemcitabine of the three pancreatic cancer cell lines was demonstrated. Indeed, after treatment with gemcitabine for 24 h, there was a modest increase in cytotoxicity by inhibition of 5′-nucleotidase and cytidine deaminase, whereas a 10-fold increase in IC_{50}, indicating suppression of cytotoxicity, was observed in all cell lines with simultaneous exposure to 2′-deoxycytidine and gemcitabine (Table 1).

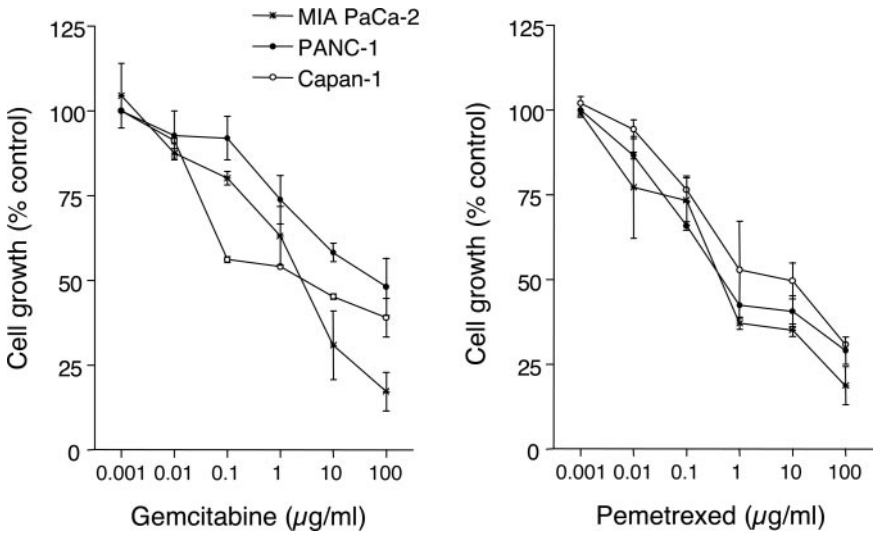

Fig. 2 Inhibitory effect of gemcitabine and pemetrexed on cell proliferation in pancreatic cancer cells. *Points*, mean values obtained from three independent experiments; *bars*, ±SE.

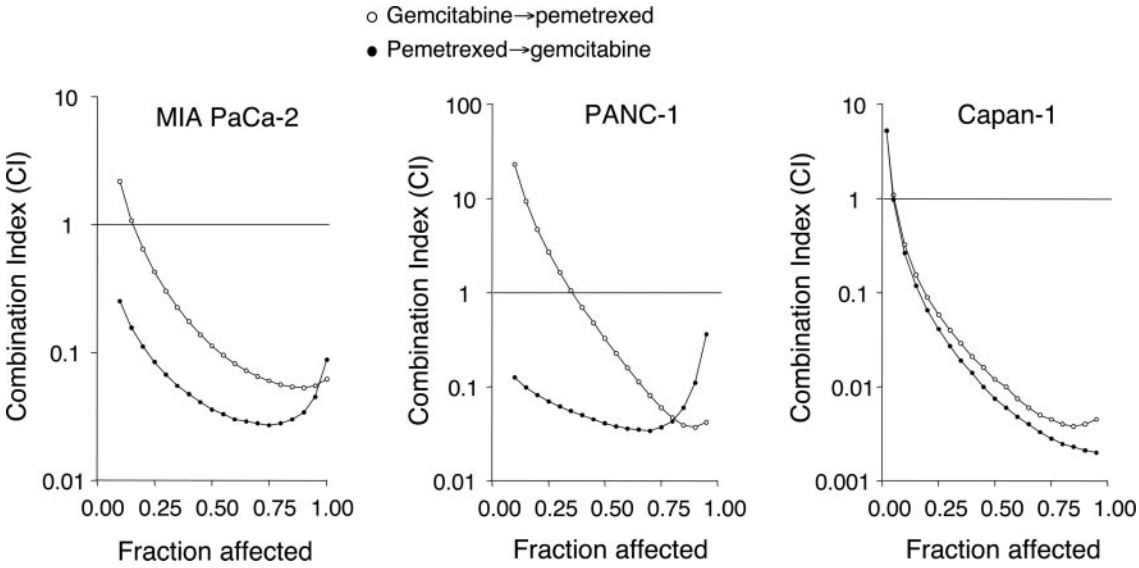

Fig. 3 Combination index (CI) plots of pemetrexed-gemcitabine combinations in MIA PaCa-2, PANC-1, and Capan-1 cells. The most pronounced synergism (CI <1) was demonstrated with the sequential administration pemetrexed→gemcitabine in Capan-1 cells.

Cell Cycle Effects of Gemcitabine and Pemetrexed. Both pemetrexed and gemcitabine were able to affect cell cycle distribution of pancreatic cancer cells (Fig. 4). In particular, the percentage of cells in S phase significantly increased ($P < 0.05$), after treatment with pemetrexed for 24 h, from 15.3 to 46.6% (MIA PaCa-2), from 10.6 to 80.1% (PANC-1), and from 31.1 to 63.2% (Capan-1). The same effect on cell cycle was observed after a 1-h treatment with gemcitabine in MIA PaCa-2 (+34.0%) and PANC-1 cells (+18.7%), whereas a modest increase was detected in Capan-1 cells (+5.3%; Table 2).

Table 1 Effects of deoxycytidine (dCyd) diethylpyrocarbonate (DEPC) and tetrahydrouridine (THU) on gemcitabine cytotoxicity after 24 h of continuous exposure

	IC_{50}[a] (ng/ml)			
	Gemcitabine	+dCyd	+DEPC	+THU
MIA PaCa-2	12.29 ± 3.89	86.11 ± 6.34	10.15 ± 2.21	7.54 ± 1.31
PANC-1	53.43 ± 6.24	503.97 ± 23.40	28.03 ± 2.07	10.52 ± 0.12
Capan-1	29.90 ± 0.66	272.53 ± 62.24	13.71 ± 0.40	9.40 ± 0.70

[a] Mean values ± SE of at least three independent experiments.

Induction of Apoptosis by Gemcitabine and Pemetrexed. Cells exposed to pemetrexed, gemcitabine, and their combination presented typical apoptotic morphology with cell shrinkage, nuclear condensation and fragmentation, and rupture of cells into debris (Fig. 5). Only 5–6% of apoptotic cells were observed after pemetrexed treatment, and a higher percentage (6–15%) was found after gemcitabine exposure in all cell lines, but the pemetrexed→gemcitabine sequential exposure significantly increased apoptotic index up to 22.0 ± 1.4%, 17.3 ±

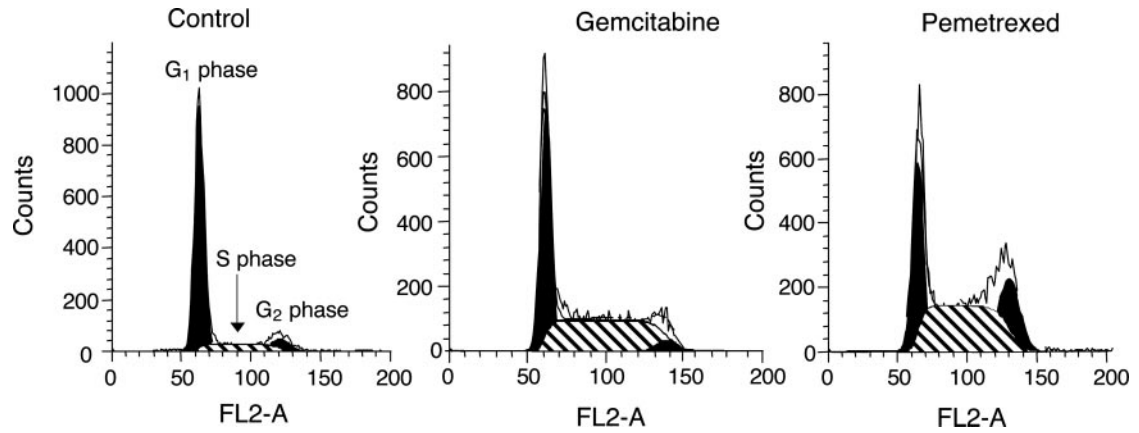

Fig. 4 Histograms of DNA content of MIA PaCa-2 cells demonstrating the accumulation of cells in S phase in a representative experiment as a consequence of treatment with gemcitabine and pemetrexed. FL2-A, fluorescence measured by FL2-A channel.

Table 2 Effect of gemcitabine and pemetrexed on cell cycle of pancreatic cancer cell lines[a]

	Treatment	G_1 (%)[a]	S phase (%)	G_2 (%)
MIA PaCa-2	Control	77.01	15.30	7.69
	Gemcitabine	46.36	49.29	4.35
	Pemetrexed	30.12	46.63	23.25
PANC-1	Control	88.25	10.55	1.20
	Gemcitabine	66.98	29.29	3.73
	Pemetrexed	17.21	80.13	2.66
Capan-1	Control	50.73	31.13	18.14
	Gemcitabine	54.19	36.40	9.41
	Pemetrexed	31.10	63.21	5.69

[a] Mean percentage values of total number of cells examined in three independent experiments.

2.6%, and 19.4 ± 1.5% in MIA PaCa-2, PANC-1, and Capan-1 cells, respectively (Fig. 5).

Inducible *dCK* Gene Expression and Correlation with Cytotoxicity. The expression of *dCK* was increased by pemetrexed up to +227.9, +86.0, and +135.5% and by gemcitabine up to 8.5, 153.1, and 55.3% in MIA PaCa-2, PANC-1, and Capan-1 cells, respectively (Fig. 6), as also demonstrated by the shift to the left of the amplification plot (Fig. 6). Because the expression of *dCK* and *RR* are thought to be involved in gemcitabine chemosensitivity, the *dCK/RRM1×RRM2* expression ratio was calculated and a correlation ($R^2 = 0.95$) was demonstrated with gemcitabine sensitivity in this panel of cells, the cell line with higher *dCK/RRM1×RRM2* value (MIA PaCa-2) being the most chemosensitive (Fig. 7). Moreover, after pemetrexed treatment, there was a marked increase in *dCK* expression and a modest up-regulation in *RRM1* and *RRM2* levels; therefore, the ratio *dCK/RRM1×RRM2* mRNA expression increased by 39.3, 12.0, and 12.3% in MIA PaCa-2, PANC-1, and Capan-1 cells respectively, potentially facilitating gemcitabine activity (Fig. 8).

Discussion

The aim of the present study was to investigate the cytotoxic activity of gemcitabine and pemetrexed in combination and to define the optimal schedule and the cellular mechanism involved in drug interaction against human pancreatic cancer cells.

In preclinical studies, the combination of pemetrexed and gemcitabine yielded conflicting results on various colorectal cancer cell lines. A recent study showed a synergistic cytotoxicity of gemcitabine followed by pemetrexed in HCT-8 cells (20), and similar results were obtained in LoVo, WiDr, and LRWZ cells, in which a higher synergistic interaction was observed with gemcitabine followed by pemetrexed, and the reverse sequence caused an additive-synergistic effect (21). On the contrary, a previous study demonstrated that the schedule-dependent synergism was maximal when pemetrexed preceded gemcitabine in HT29 cells (16). In agreement with these findings, *in vitro* experimental data obtained in this study indicate that pemetrexed and gemcitabine interacted synergistically against MIA PaCa-2, PANC-1, and Capan-1 cells, and the highest chemotherapeutic activity was observed with the sequence pemetrexed→gemcitabine.

Recent studies have shown the importance of modulating

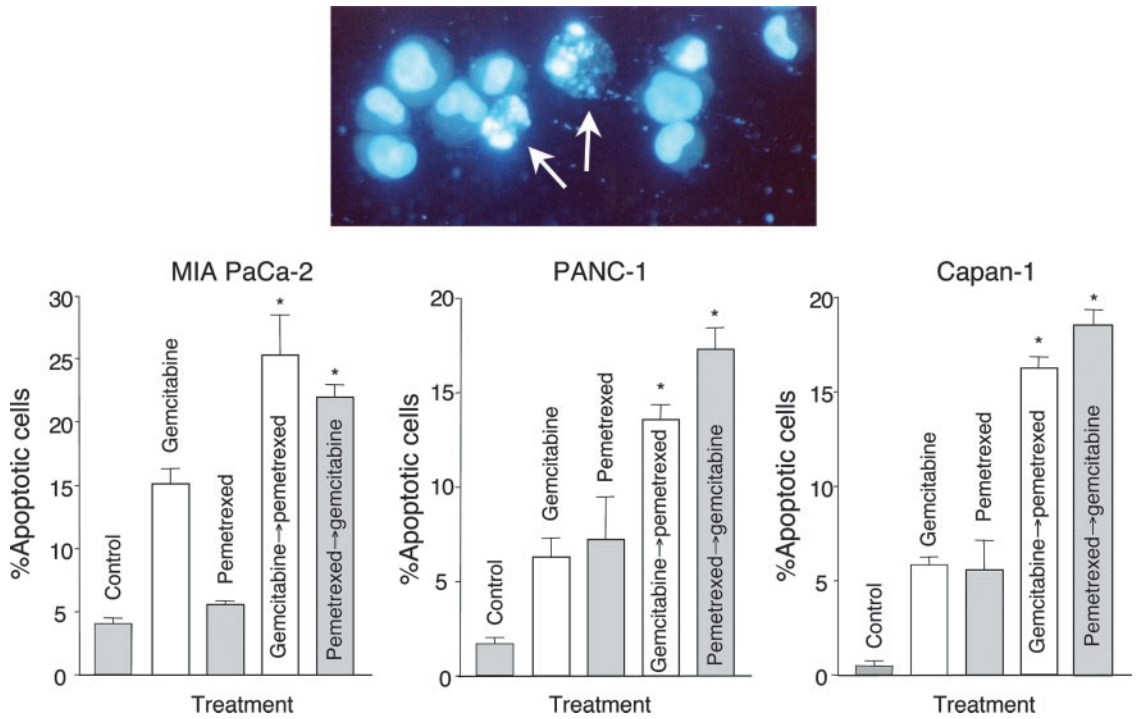

Fig. 5 Induction of apoptosis by gemcitabine, pemetrexed, and their combinations. *Inset panel*, morphological appearance of apoptotic cells. *Columns*, mean values obtained from three independent experiments; *bars*, SE; *, statistically significantly different from controls ($P < 0.05$).

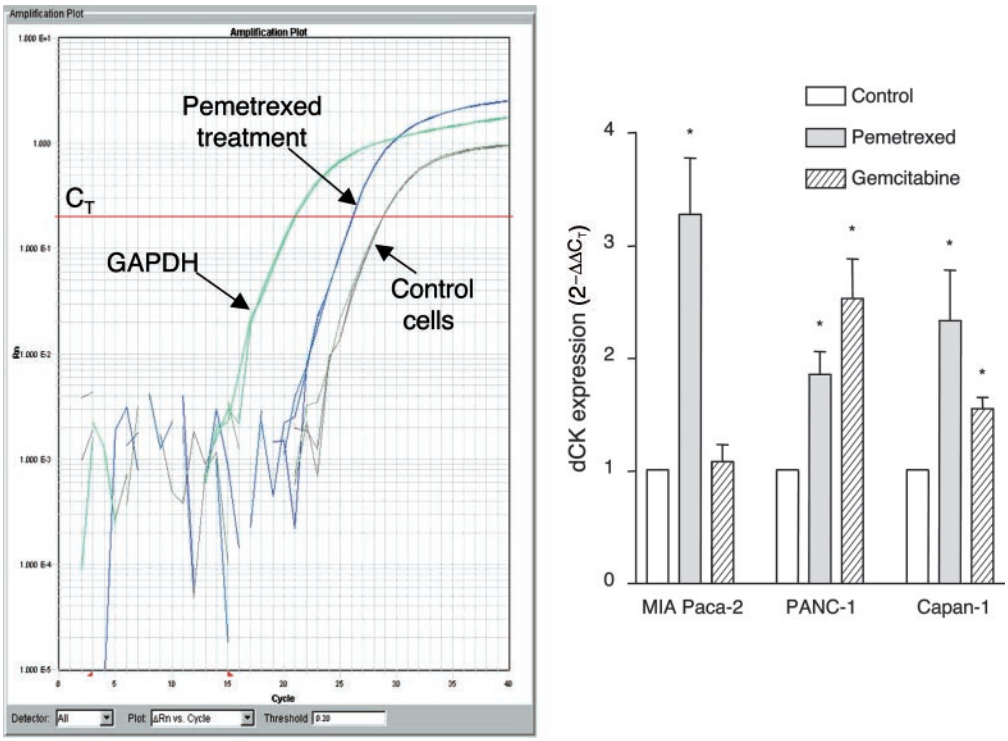

Fig. 6 *Left panel*, Representative plot of deoxycytidine kinase (*dCK*) and glyceraldehyde 3-phosphate dehydrogenase (*GAPDH*) amplification in MIA PaCa-2 cells showing the up-regulation of dCK expression by pemetrexed in comparison with control cells. *Right panel*, dCK expression in MIA PaCa-2, PANC-1, and Capan-1 pancreatic cancer cells. *Columns*, mean values obtained from two independent experiments; *bars*, ±SE; ∗, statistically significantly different from control cells ($P < 0.05$).

the cell cycle to exploit the effect of drug combinations (8, 22). In the present study, flow cytometry demonstrated that both pemetrexed and gemcitabine caused an accumulation of cells in S phase, as a result of the inhibition of DNA synthesis. This finding is in agreement with previous data on increased proportion of MIA PaCa-2 cells in S phase after gemcitabine treatment (23), and on the accumulation of CCRF-CEM and HT29 cells in S phase after 12–24 h of exposure to pemetrexed (15, 16). Because gemcitabine is a S-phase-specific drug, the increase in its activity in the schedule pemetrexed→gemcitabine may be the result of a modulation of cell cycle potentially facilitating 2′,2′-difluoro-dCTP incorporation in DNA.

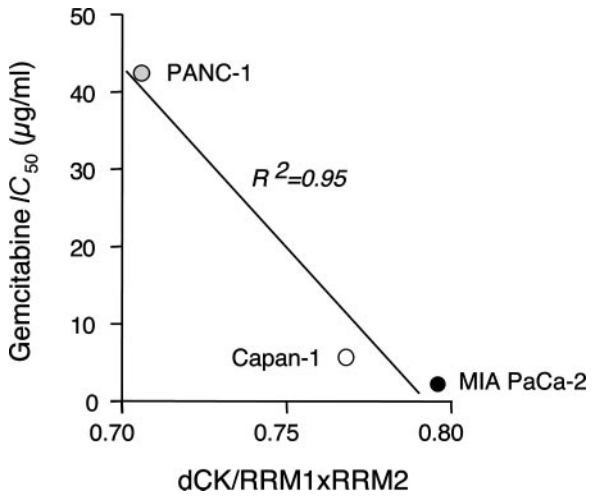

Fig. 7 Correlation of the deoxycytidine kinase *dCK RRM1* (regulatory subunit of ribonucleotide reductase) ×*RRM2* (catalytic subunit of ribonucleotide reductase) expression ratio with gemcitabine chemosensitivity (IC_{50} after 1-h treatment) in MIA PaCa-2, PANC-1 and Capan-1 cells. *Points*, mean values obtained from three independent experiments.

Deregulation of apoptosis machinery might explain the resistance of cancer cells to chemotherapeutic agents, and a recent study showed that the up-regulation of the phosphatidylinositol-3′-kinase-AKT cell survival pathway correlated with impairment of gemcitabine-induced apoptosis and antitumor activity in human pancreatic adenocarcinoma PK1 and PK8 cells (24). Therefore, not only impaired drug uptake, but also the loss of ability to undergo apoptosis may be involved in gemcitabine resistance (25). Thus, the development of drug combinations that increase apoptosis represents an important approach for the rational design of treatment schedules. In particular, the combination with pemetrexed may improve the therapeutic activity of gemcitabine by increasing the activation of the apoptotic pathway. In the present *in vitro* study MIA PaCa-2, PANC-1, and Capan-1 cells were exposed to the gemcitabine and pemetrexed in combination at their IC_{50} levels, and a significant enhancement of apoptosis in treated cells was observed when compared with control cells. A similar observation has been reported in the colon cancer cell line WiDr, with which

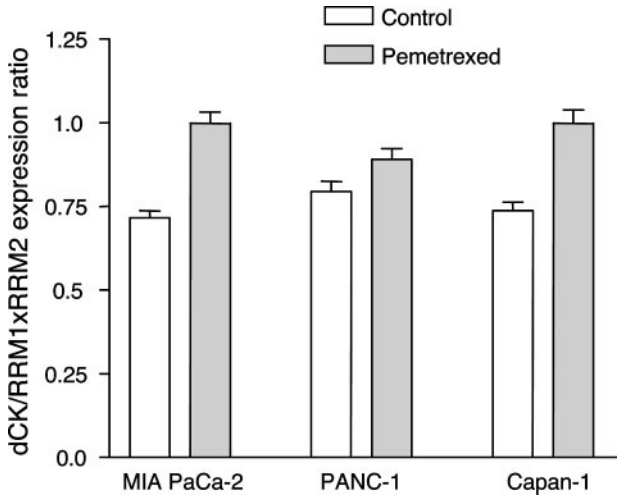

Fig. 8 Enhancement of deoxycytidine kinase *dCK RRM1* (regulatory subunit of ribonucleotide reductase) ×*RRM2* (catalytic subunit of ribonucleotide reductase) expression ratio after pemetrexed treatment in MIA PaCa-2, PANC-1, and Capan-1 cells. *Columns*, mean values obtained from three independent experiments; *bars*, SE.

only 1% of apoptotic cells were observed after gemcitabine treatment, whereas a higher percentage was found after gemcitabine–pemetrexed combination (21).

Several observations have suggested that dCK, a key enzyme of the nucleoside salvage pathway, is a limiting factor for the antitumor effect of gemcitabine because its activity is often decreased in cells resistant to nucleoside analogs, and the sensitivity to these drugs could be restored by transfection with a wild-type *dCK* (26, 27). Recent studies also showed a clear correlation between *dCK* expression and gemcitabine sensitivity in human tumor xenografts (28); in agreement with these findings, the crucial role of dCK was confirmed in the present work by the 10-fold increase in the IC_{50} in gemcitabine with 2′-deoxycytidine in MIA PaCa-2, PANC-1, and Capan-1 cells. Because pemetrexed inhibits various enzymes, including glycinamide ribonucleotide formyltransferase, which catalyzes the first reaction in *de novo* purine biosynthesis (13, 29), treatment with this drug could increase the expression of *dCK* as a compensatory mechanism. The present study confirmed this hypothesis and suggested the potential predictive value of the *dCK/RRM1*×*RRM2* expression ratio with respect to chemosensitivity to gemcitabine. Therefore, the up-regulation of *dCK* by pemetrexed, without a parallel increase in *RR* expression, and the favorable modulation of cell cycle may be considered the most important mechanisms underlying the synergistic interaction with gemcitabine. Two potential applications of these findings may be thus envisaged: (*a*) integration of pemetrexed in gemcitabine combination regimens to increase drug activity and restore chemosensitivity in tumor cells with *dCK* down-regulation; and (*b*) application of pharmacogenetic profiling to assess the potential tumor cell sensitivity to gemcitabine.

Finally, an increase in *dCK* expression was also observed after gemcitabine exposure in PANC-1 and Capan-1 cells, and this result is in agreement with previous studies demonstrating that the salvage pathway initiated by dCK accounted for the majority of nucleotide synthesis for DNA repair (30), particularly after treatment with antimetabolites (31).

In conclusion, this study characterizes the synergistic effect between gemcitabine and pemetrexed against *in vitro* models of pancreatic cancer and the potential mechanisms involved, and provides the experimental basis for the rational development of this combination for the treatment of this malignancy.

References

1. Oettle H, Riess H. Gemcitabine in combination with 5-fluorouracil with or without folinic acid in the treatment of pancreatic cancer. Cancer (Phila) 2002;95:912–22.

2. Philip PA. Gemcitabine and platinum combinations in pancreatic cancer. Cancer (Phila) 2002;95:908–11.

3. Peters GJ, van der Wilt CL, van Moorsel CJ, Kroep JR, Bergman AM, Ackland SP. Basis for effective combination cancer chemotherapy with antimetabolites. Pharmacol Ther 2000;87:227–53.

4. van Moorsel CJ, Pinedo HM, Veerman G, et al. Mechanism of synergism between cisplatin and gemcitabine in ovarian and non-small-cell lung cancer cell lines. Br J Cancer 1999;80:981–90.

5. Edelman MJ, Quam H, Mullins B. Interactions of gemcitabine, carboplatin and paclitaxel in molecularly defined non-small-cell lung cancer cell lines. Cancer Chemother Pharmacol 2001;48:141–4.

6. Symon Z, Davis M, McGinn CJ, Zalupski MM, Lawrence TS. Concurrent chemoradiotherapy with gemcitabine and cisplatin for pancreatic cancer: from the laboratory to the clinic. Int J Radiat Oncol Biol Phys 2002;53:140–5.

7. Tolis C, Peters GJ, Ferreira CG, Pinedo HM, Giaccone G. Cell cycle disturbances and apoptosis induced by topotecan and gemcitabine on human lung cancer cell lines. Eur J Cancer 1999;35:796–807.

8. Theodossiou C, Cook JA, Fisher J, et al. Interaction of gemcitabine with paclitaxel and cisplatin in human tumor cell lines. Int J Oncol 1998;12:825–32.

9. Zoli W, Ricotti L, Dal Susino M, et al. Docetaxel and gemcitabine activity in NSCLC cell lines and in primary cultures from human lung cancer. Br J Cancer 1999;81:609–15.

10. Noble S, Goa K. Gemcitabine, a review of its pharmacology and clinical potential in non-small cell lung cancer and pancreatic cancer. Drugs 1997;54:447–72.

11. Gandhi V, Mineishi S, Huang P. Cytotoxicity, metabolism and mechanism of action of 2′,2′-difluoro-deoxyguanosine in the Chinese hamster ovary cells. Cancer Res 1995;55:1517–24.

12. Bergman AM, Pinedo HM, Peters GJ. Determinants of resistance to 2′,2′-difluorodeoxycytidine (gemcitabine). Drug Resist Upd 2002;5:19–33.

13. Shih C, Chen VJ, Gossett LS, et al. LY231514, a pyrrolo[2,3-d]pyrimidine-based antifolate that inhibits multiple folate-requiring enzymes. Cancer Res 1997;57:1116–23.

14. Chen VJ, Bowley JR, Andis SL, et al. Cellular pharmacology of MTA: a correlation of MTA-induced cellular toxicity and in vitro enzyme inhibition with its effects on intracellular folate and nucleoside triphosphate pools in CCRF-CEM cells. Semin Oncol 1999; 26:48–54.

15. Tonkinson JL, Marder P, Andis SL, et al. Cell cycle effects of antifolate antimetabolites implications for cytotoxicity and cytostasis. Cancer Chemother Pharmacol 1997;39:521–31.

16. Tonkinson JL, Worzalla JF, Teng CH, Mendelsohn LG. Cell cycle modulation by a multitargeted antifolate, LY231514, increases the cytotoxicity and antitumor activity of gemcitabine in HT29 colon carcinoma. Cancer Res 1999;59:3671–6.

17. Chou TC, Motzer R, Tong Y, Bosl G. Computerized quantitation of synergism and antagonism of Taxol, topotecan, and cisplatin against human teratocarcinoma cell growth: a rational approach to clinical protocol design. J Natl Cancer Inst (Bethesda) 1994;86:1517–24.

18. Hsueh CT, Chiu CF, Kelsen DP, Schwartz GK. Selective inhibition of cyclooxygenase-2 enhances mitomycin-C-induced apoptosis. Cancer Chemother Pharmacol 2000;45:389–96.

19. Mocellin S, Rossi CR, Pilati P, Nitti D, Marincola FM. Quantitative real-time PCR: a powerful ally in cancer research. Trends Mol Med 2003;9:189–95.

20. Adjei AA, Erlichman C, Sloan AJ, et al. Phase I and pharmacologic study of sequences of gemcitabine and the multitarget antifolate agent in patients with advanced solid tumors. J Clin Oncol 2000;8:1748–57.

21. Tesei A, Ricotti L, De Paola F, Amadori D, Frassinetti GL, Zoli W. In vitro schedule-dependent interactions between the multitarget antifolate LY231514 and gemcitabine in human colon adenocarcinoma cell lines. Clin Cancer Res 2002;8:233–9.

22. Zoli W, Ricotti L, Barzanti F, et al. Schedule-dependent interaction of doxorubicin, paclitaxel and gemcitabine in human breast cancer cell lines. Int J Cancer 1999;80:413–6.

23. Yip-Schneider MT, Sweeney CJ, Jung SH, Crowell PL, Marshall MS. Cell cycle effects of nonsteroidal anti-inflammatory drugs and enhanced growth inhibition in combination with gemcitabine in pancreatic carcinoma cells. J Pharmacol Exp Ther 2001;298:976–85.

24. Ng SSW, Tsao MS, Chow S, Hedley DW. Inhibition of phosphatidylinositide 3-kinase enhances gemcitabine-induced apoptosis in human pancreatic cancer cells. Cancer Res 2000;60:5451–5.

25. Mackey JR, Mani RS, Selnerm M, et al. Functional nucleoside transporters are required for gemcitabine influx and manifestations of toxicity in cancer cell lines. Cancer Res 1998;58:4349–57.

26. Gregoire V, Rosier JF, De Bast M, et al. Role of deoxycytidine kinase (DCK) activity in gemcitabine's radioenhancement in mice and human cell lines in vitro. Radiother Oncol 2002;63:329–38.

27. Hapke DM, Stegmann AP, Mitchell BS. Retroviral transfer of deoxycytidine kinase into tumor cell lines enhances nucleoside toxicity. Cancer Res 1996;56:2343–7.

28. Kroep JR, Loves WJ, van der Wilt CL, et al. Pretreatment deoxycytidine kinase levels predict in vivo gemcitabine sensitivity. Mol Cancer Ther 2002;1:371–6.

29. Chong LK, Tattersall MH. 5,10-Dideazatetrahydrofolic acid reduces toxicity and deoxyadenosine triphosphate pool, expansion in cultured L1210 cells treated with inhibitors of thymidylate synthase. Biochem Pharmacol 1995;49:819–27.

30. Iwasaki H, Huang P, Keating MJ, Plunkett W. Differential incorporation of ara-C, gemcitabine, and fludarabine into replicating and repairing DNA in proliferating human leukemia cells. Blood 1997;90:270–8.

31. Sasvari-Szekely M, Csapo Z, Spasokoukotskaja T, Eriksson S, Staub M. Activation of deoxycytidine kinase during inhibition of DNA synthesis in human lymphocytes. Adv Exp Med Biol 1998;431:519–23.